First-in-human diagnostic study of hepatic steatosis with computed ultrasound tomography in echo mode (CUTE)

Patrick Stähli
University of Bern
Chiara Becchetti
Inselspital, Bern University Hospital
Naiara Korta Martiartu
University of Bern https://orcid.org/0000-0002-7970-7900
Annalisa Berzigotti
University Hospital of Bern
Martin Frenz
University of Bern https://orcid.org/0000-0002-6741-9434
Michael Jaeger (michael.jaeger@unibe.ch)
University of Bern

Article

Keywords:

Posted Date: September 6th, 2022

DOI: https://doi.org/10.21203/rs.3.rs-1920871/v1

First-in-human diagnostic study of hepatic steatosis with computed ultrasound tomography in echo mode (CUTE)

Patrick Stähli[1,4], Chiara Becchetti[2,4], Naiara Korta Martiartu[1,4], Annalisa Berzigotti[2, 3], Martin Frenz[1], and Michael Jaeger[1,*]

[1]Institute of Applied Physics, University of Bern, Bern, Switzerland.
[2]Department of Visceral Surgery and Medicine, Inselspital, Bern University Hospital, University of Bern, Bern, Switzerland.
[3]Department of Biomedical Research, University of Bern, Bern, Switzerland.
[4]These authors contributed equally.
[*]email: michael.jaeger@unibe.ch

Abstract

Non-alcoholic fatty liver disease is rapidly emerging as the leading global cause of chronic liver disease. Efficient disease management requires low-cost, noninvasive techniques for diagnosing hepatic steatosis accurately. Here we propose quantifying liver speed-of-sound (SoS) with computed US tomography in echo mode (CUTE), a newly developed US imaging modality adapted to clinical pulse-echo systems. CUTE reconstructs the spatial distribution of SoS by measuring local echo phase shifts when probing tissue at different steering angles in transmission and reception. This first-in-human phase II study shows that liver CUTE-SoS estimates correlate strongly ($r = -0.84, p = 8.27 \cdot 10^{-13}$) with controlled attenuation parameter values, a commonly used tool for assessing liver steatosis, and have 90.9% (95% confidence interval: 84 - 100%) sensitivity and 95.5% (81 - 100%) specificity for differentiating normal and significantly steatotic livers. Because CUTE offers the same flexibility as conventional US imaging, it can be readily extended to other clinical applications, establishing it as a new quantitative add-on to diagnostic US.

Introduction

Non-alcoholic fatty liver disease (NAFLD) is currently the most prevalent type of chronic liver disease, with an estimated number of one billion affected individuals worldwide [1, 2, 3]. NAFLD is characterized by steatosis, namely the accumulation of fat in the liver, and its aggressive form (non-alcoholic steatohepatitis) may progress to liver fibrosis, cirrhosis, and eventually hepatocellular carcinoma [4]. Early diagnosis of hepatic steatosis is crucial to prevent the development of advanced disease stages. In this regard, liver biopsy and magnetic resonance (MR) are the gold standards, although both become inefficient and inadequate for large-scale screening that the increasing prevalence of NAFLD requires [5]. Developing cost-effective non-invasive diagnostic methods is therefore a high clinical and research priority.

Ultrasound (US) imaging systems possess essential qualities to tackle the challenges of screening for NAFLD. They are safe, relatively inexpensive, readily available in most clinical facilities, and provide real-time feedback. In fact, US is commonly employed to assess hepatic steatosis by analyzing features in conventional gray-scale B-mode images such as the echo intensity, distribution, and contrast [6, 7]. Unfortunately, these parameters are qualitative, and their assessment strongly depends on the expertise of the sonographer [8]. Such subjective evaluation makes the sensitivity of conventional US particularly poor (60.9%-65%) for low-grade hepatic steatosis ($\leq$ 20% fat content) [9, 10, 6].

Quantitative indicators of steatosis are indispensable to improving the sensitivity and diagnostic accuracy of US. The fat accumulation alters the liver composition and, consequently, its acoustic and mechanical

properties, which we can quantify from US radio-frequency signals. For example, the energy loss or attenuation that US waves undergo during their propagation through the liver increases in the presence of fat [11] and can be used as an indicator of steatosis. With this idea in mind, the controlled attenuation parameter (CAP) has been developed using vibration-controlled transient elastography on FibroScan equipment (Echosens, Paris, France) [12]. CAP estimates the average US attenuation in a cylindrical volume of the liver of approximately 1 cm diameter at 25-65 mm depth using 3.5 MHz M probes (or at 35–75 mm depth with 2.5 MHz XL probes) [13] and shows significant correlations with histological steatosis grades (Spearman correlation coefficient: 0.81, $p < 10^{-16}$) [14, 15, 12]. Despite emerging as a widely used non-invasive diagnostic tool, CAP measurements depend substantially on covariates such as aetiology, diabetes status, or body mass index, bringing concerns about its diagnostic performance [16, 17].

Quantifying other tissue properties sensitive to composition could complement CAP measurements to improve its diagnostic ability. A promising candidate is the propagation velocity of longitudinal US waves in tissue, referred to as the speed of sound (SoS), which decreases considerably with fat content [18, 19, 20]. A recent clinical study in a population with different grades of steatosis has shown encouraging results with excellent correlations between average liver SoS estimates and MR-based fat-fraction measurements [21]. However, these average SoS measurements do not capture the intrinsic tissue heterogeneity and require a manual correction with assumed values of the SoS distribution in the abdominal wall [19, 22], making them prone to biases. This limitation can be efficiently overcome with tomography techniques that directly reconstruct the spatial distribution of tissue SoS in the field of view of US images. For this purpose, we have developed the computed ultrasound tomography in echo mode (CUTE) technique, which allows us to image tissue SoS using conventional hand-held pulse-echo US systems [23, 24, 25, 26]. CUTE reconstructs the spatial distribution of tissue SoS by measuring local echo phase shifts caused by SoS heterogeneities when probing tissue at different steering angles in transmission and reception (Fig. 1). This is practically equivalent to having a virtual receiver that measures time delays between specific wave-propagation paths at every spatial location. So far, CUTE has proven excellent in retrieving correct SoS values with approximately 10 m/s contrast resolution in tissue-mimicking phantoms [27], opening up the prospect of quantitative non-invasive diagnosis with SoS imaging.

This study investigates the performance of CUTE-based liver SoS estimates (CUTE-SoS) for diagnosing hepatic steatosis in a single-center, investigator-initiated, cross-sectional, first-in-human phase II clinical study. Specifically, we focus on evaluating the ability of CUTE-SoS to differentiate normal livers from those diagnosed with significant or severe steatosis ($\geq$33% fat content) using CAP measurements as a reference (cut-off $\geq$280 dB/m [17]). For this, we use the SuperSonic® MACH® 30 US system with C6-1X probe (Hologic® - Supersonic Imagine®, Aix en Provence, France) to collect US radio-frequency signals and develop a fully-integrated convex-probe CUTE implementation to reconstruct SoS (see Methods for further details).

Results

Study participants

In this study, we evaluated the liver of 44 participants, of which 22 had significant or severe steatosis confirmed with conventional US B-mode images and CAP. Their median (range) age and body mass index were 37 (24 - 77) years and 26 (19 - 38) kg/m^2, respectively. Participants with significant or severe liver steatosis were older (mean 47 years vs. 34 years, $p = 0.002$) and more obese (30 kg/m^2 vs. 23 kg/m^2, $p = 2.8 \cdot 10^{-10}$) than their healthy counterparts (Table 1).

Reference standard CAP measurements

Fatty liver patients were recruited at a regular screening visit if their CAP values measured with the Fibroscan system either with M or XL probe exceeded 280 dB/m. For consistency, CAP measurements

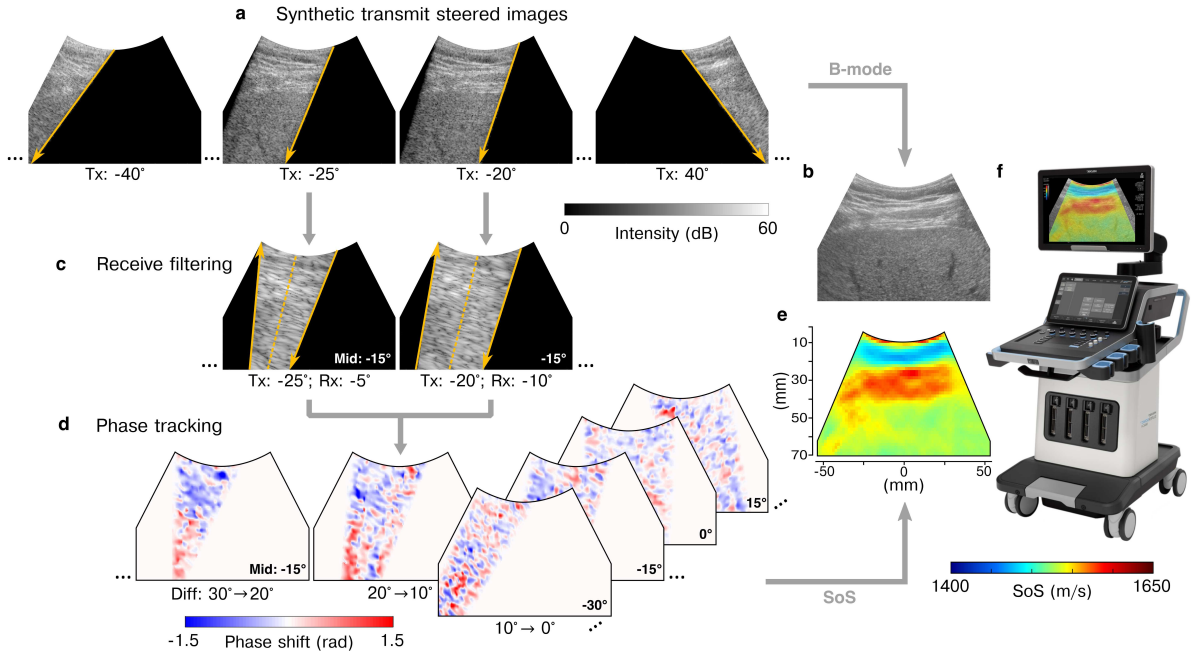

Figure 1: Computed ultrasound tomography in echo mode (CUTE) workflow. **a** Tissue is insonified by sequentially transmitting a set of wavefronts with varying steering angles. We use delay-and-sum beamforming and coherent compounding on the recorded radio-frequency signals to reconstruct synthetically focused and steered ultrasound images for transmit (Tx) angles ranging from $-55°$ to $55°$ relative to the axial direction. Orange downwards-pointing arrows indicate the orientation of these Tx wavefronts. **b** We combine all these images to form a conventional echo-intensity B-mode image. **c** For CUTE, each image in **a** is decomposed via spatial frequency filtering into a set of images corresponding to different receive (Rx) steering angles (orange upwards-pointing arrows). These images are characterized by the mid angle (Mid) between Tx and Rx angles (dashed orange lines). Tx-Rx angle pairs with identical mid-angle provide well-correlated images. **d** We extract the spatial distribution of echo phase shifts from such well-correlated image pairs. We obtain a phase-shift map per mid angle and Tx-Rx angle difference (Diff). **e** Tissue speed of sound (SoS) is estimated from phase-shift maps solving a linear inverse problem. **f** The result is displayed together with the B-mode image in the SuperSonic® MACH® 30 ultrasound system. Although CUTE uses complex radio-frequency images in steps **a** and **c**, here we show echo-intensity images for illustrative purposes.

for this study were acquired in a second visit, right before US data acquisition for CUTE-SoS. Although all patients had CAP $\geq$ 280 dB/m at the time of recruitment, one patient showed values below this threshold in the second visit (267 dB/m, Supplementary Table 1). Still, the patient was included in the study because feature analysis in conventional US B-mode images confirmed significant steatosis. The median of ten CAP measurements per participant ranged from 267 dB/m to 394 dB/m and from 160 dB/m to 238 dB/m for steatotic and normal livers, respectively (mean 333 dB/m vs. 195 dB/m, $p = 7.16 \cdot 10^{-09}$, Table 1).

CUTE-SoS images

US radio-frequency signals were acquired by a physician blinded to CUTE-SoS images to avoid biases. From a total of 220 acquisitions (five per patient), three resulted in empty datasets (1.4%), probably due to a systemic failure in the data storage process. Acquired radio-frequency signals were then used by a researcher blinded to characteristics of participants and CAP values to reconstruct CUTE-SoS images and extract liver SoS.

Fig. 2 shows examples of B-mode and CUTE-SoS images in a normal and steatotic liver (all images in Supplementary Fig. 1). The two types of images display different tissue properties with complementary

Table 1: Characteristics of study population.

	Healthy n = 22	**Steatotic n = 22**
Age (years)		
Mean (SD)	34 (10)	47 (15)
Min, max	24, 58	24, 77
Sex-n		
Female (%)	14 (63.6)	6 (27.3)
Male (%)	8 (34.4)	16 (72.7)
Weight (kg)		
Mean (SD)	70 (12)	94 (16)
Min, max	50, 99	65, 124
BMI (kg/m^2)		
Mean (SD)	23 (2)	30 (4)
Min, max	19, 28	25, 38
CAP (dB/m)		
Mean (SD)	195 (26)	333 (28)
Min, max	160, 238	267, 394

BMI body mass index

CAP controlled attenuation parameter

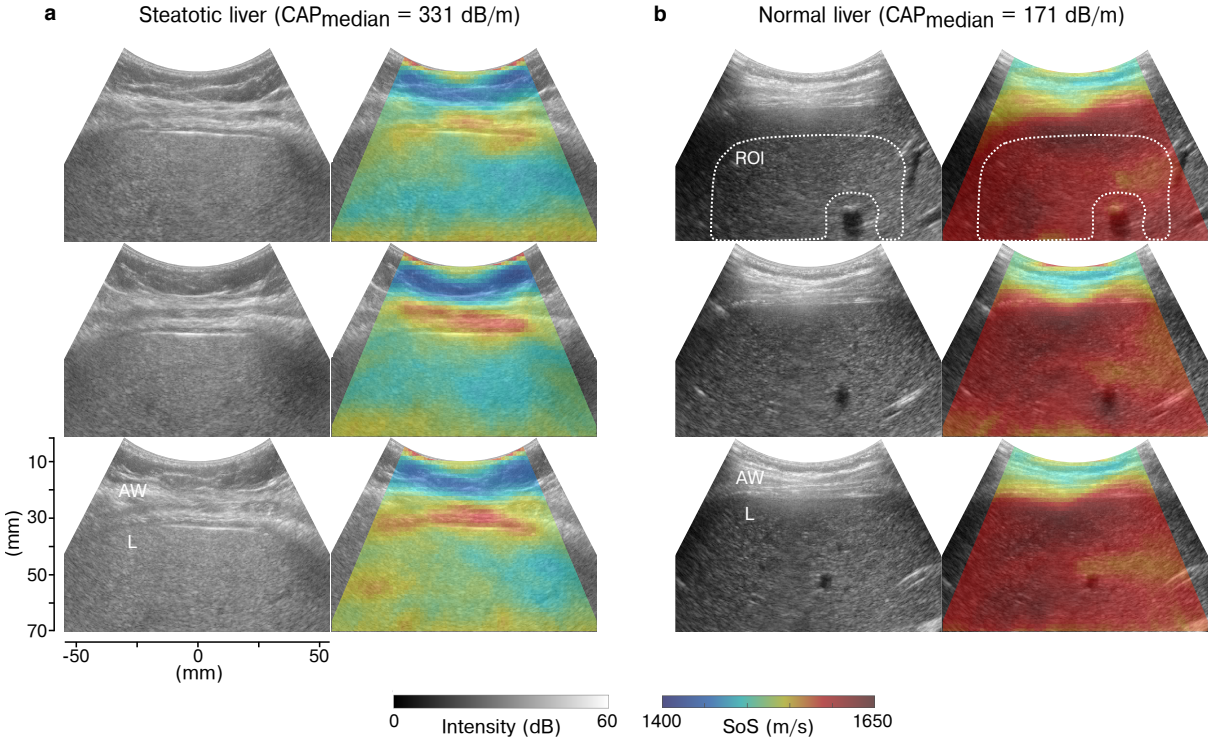

Figure 2: Example images of ultrasound B-mode and CUTE speed of sound in a normal and steatotic liver. **a, b** Echo intensity (left column) and speed-of-sound (SoS) distribution (right column) in a steatotic and normal liver with median controlled attenuation parameter (CAP) values of 331 dB/m and 171 dB/m, respectively. In each case, we show images corresponding to three distinct data acquisitions (rows) to illustrate the repeatability of CUTE-SoS and the correspondence between structures in B-mode and CUTE-SoS images. The first row in **b** shows an example of the manually selected region of interest (ROI) with blood vessels (dark areas) excluded, from which we extracted the mean liver SoS value. AW: abdominal wall; L: liver.

physiological and structural information. Reconstructed CUTE-SoS images show excellent axial resolution, capturing the SoS distribution of the abdominal wall and liver. The axial resolution is particularly high in the shallowest region, as suggested by the spatial correspondence between the reconstructed subcutaneous fat-intercostal muscle interface (low and high SoS, respectively) in B-mode and CUTE-SoS images (Fig. 2a). In contrast, the liver capsule generally appears more diffused, probably caused by tissue composition and architecture complexity of the abdominal wall region. This intercostal space contains muscles, connective tissues, fat inclusions, and highly reflective interfaces, which may introduce reverberation artifacts similar to those observed in elastography [28], resulting in unreasonable SoS values within approximately the first 10 mm below the liver capsule. In the liver, fat accumulation reduces SoS values; thus, reconstructed SoS is generally lower in steatotic livers than in normal ones. In some cases, we observe large blood vessels that appear anechoic (dark) in B-mode images (Fig. 2b). Measured echo phase shifts within these regions are unreliable [29] and may generate SoS artifacts inside and around the vessels (e.g., the lower SoS area on top of the blood vessels in Fig. 2b).

Liver SoS

We extracted mean liver SoS values and corresponding standard deviations (Supplementary Table 1) by manually selecting regions of interest (ROI) that exclude the first 10 mm below the liver capsule and areas surrounding large blood vessels with approximately 5 mm extension to avoid reconstruction artifacts (Fig. 2b and Supplementary Fig. 1). The reliability of repeated mean SoS measurements (Supplementary Table 2) was excellent, with the intraclass correlation coefficient ranging between 0.95 and 0.98 ($p = 4.08 \cdot 10^{-58}$). Whereas patients with liver steatosis had significantly larger CAP values than healthy individuals (Fig. 3a), their mean liver SoS values were significantly lower (1543 m/s vs. 1584 m/s, $p = 4.08 \cdot 10^{-08}$), ranging from 1520 m/s to 1571 m/s and from 1551 m/s to 1608 m/s for steatotic and normal livers, respectively (Fig. 3b). CAP and SoS values were therefore negatively and significantly correlated ($r = -0.84, p = 8.27 \cdot 10^{-13}$) (Fig. 3c), meaning that both parameters are sensitive to variations in tissue composition. The mean variability of SoS within the ROI did not reveal any significant difference between the two groups ($p = 0.21$), ranging from 6 m/s to 13 m/s for steatotic livers and from 7 m/s to 13 m/s for normal ones (Supplementary Table 2). The average standard deviation was 10 m/s, in agreement with the contrast resolution observed in previous works [27].

The receiver operating characteristic (ROC) curve analysis showed excellent diagnostic performance of CUTE-SoS for identifying significant steatosis in the liver (Fig. 3d), with an area under the curve (AUC) of 0.97 (95% confidence interval (CI): 0.93 - 1.0). The optimum SoS cute-off was 1567 m/s (95% CI: 1558 - 1573 m/s), which had a sensitivity of 90.9% (95% CI: 84 - 100%) and specificity of 95.5% (95% CI: 81 - 100%) for identifying patients with liver steatosis.

Discussion

This first-in-human phase II study demonstrates that CUTE-SoS is an excellent quantitative biomarker for diagnosing significant liver steatosis non-invasively. CUTE is a newly developed US imaging modality capable of reconstructing the spatial distribution of tissue SoS using conventional handheld pulse-echo systems. It can thus be easily implemented in clinical US systems complementing other well-established modalities such as echo-intensity B-mode imaging, Doppler flow imaging, and US elastography. CUTE images allow efficient quantification of liver SoS by manually selecting a ROI within the organ guided by B-mode images to avoid reverberation and blood-vessel artifacts, offering a flexible diagnostic tool for physicians.

In this first clinical evaluation of CUTE technology, we use CAP measurements as the reference standard for differentiating normal and significantly steatotic livers, for which CAP shows particularly good diagnostic performance [15]. We observe a very strong inverse correlation between CUTE-SoS and CAP values, consistent with the fact that US waves propagate slower and attenuate more in tissue with increased fat content. Consequently, CUTE-SoS shows high sensitivity (90.9%) and specificity (95.5%) for distinguishing the two cohorts with a threshold SoS value of 1567 m/s. The seemingly reduced discriminating power of CUTE-SoS compared to CAP in Figs. 3a and 3b does not necessarily indicate an inferior

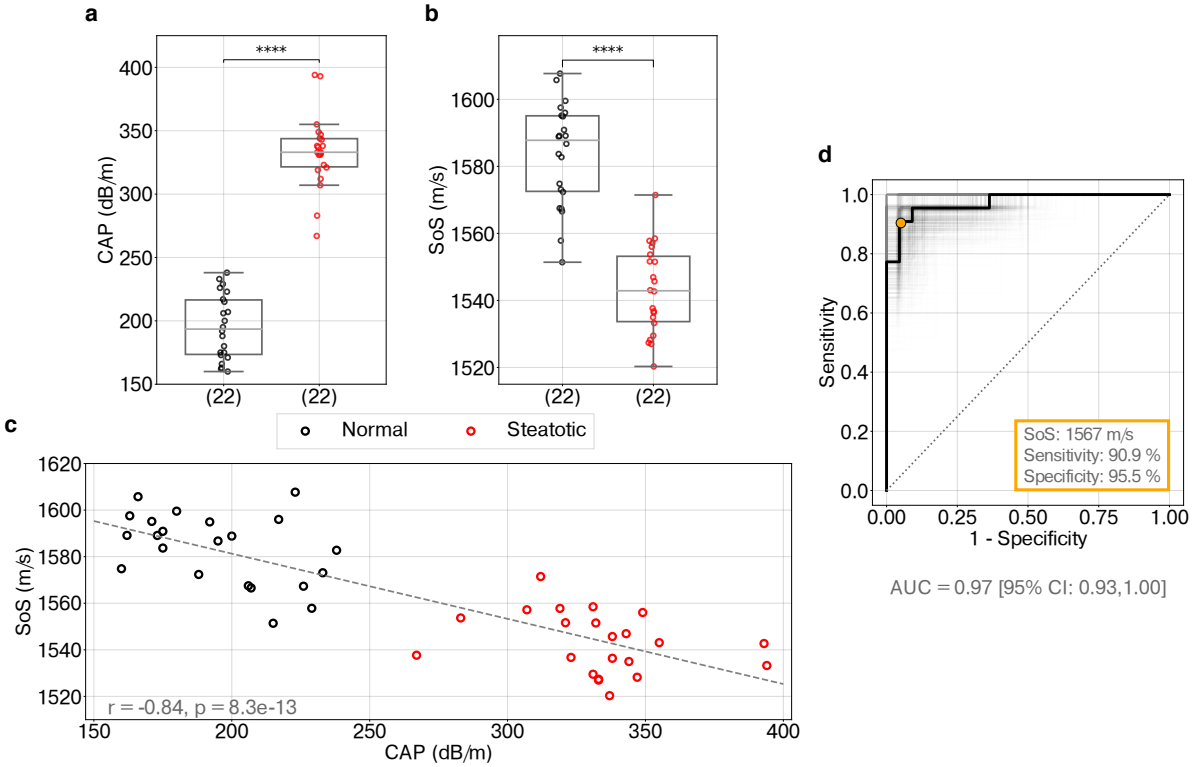

Figure 3: Diagnostic performance of CUTE speed of sound. **a** Distribution of controlled attenuation parameter (CAP) and (**b**) speed-of-sound (SoS) values in normal (n = 22) and steatotic (n = 22) livers. Box boundaries represent the first and third quartiles, the line across the box shows the median, and whiskers indicate the minimum and maximum values excluding outliers (values beyond 1.5 × inter-quartile range). The significance of differences between distributions is assessed with two-tailed Mann-Whitney U test, where **** refers to $p < 0.0001$. **c** Correlation between CAP and SoS values using Pearson's r coefficient. **d** Receiver operating characteristic (ROC) curve representing true-positive rates (sensitivity) against false-positive rates (1 − specificity) of predicting steatotic versus normal livers based on SoS values. The diagonal line indicates random prediction. The confidence interval (CI) is computed with bootstrapping, illustrated as different realizations of ROC curves in gray. AUC: Area under the curve.

diagnostic accuracy. CAP itself is expected to show some uncertainty in correctly discriminating normal vs. significantly steatotic livers. However, here we use it as the reference standard, and an artificially perfect diagnostic performance compared to CUTE is expected. To assess the full extent of the clinical utility of CUTE, a comparison with Dixon MR imaging, the reference imaging method for quantifying hepatic steatosis, may be more appropriate than CAP. Future studies will focus on this comparison to analyze the ability of CUTE to grade steatosis and monitor changes over time.

Although the accuracy of absolute CUTE-SoS values is difficult to evaluate without knowing the ground truth values, liver CUTE-SoS estimates are in excellent agreement with SoS measurements in excised human livers reported in the literature. For normal livers, reported values range from 1560 m/s to 1607 m/s [30, 31, 32], whereas CUTE-SoS values in this study range from 1551 m/s to 1608 m/s. These values decrease in steatotic livers, where the minimum reported SoS value is 1522 m/s [30] compared to the 1520 m/s that we estimate. This consistency suggests that CUTE can estimate the correct liver SoS value, which is key to quantifying the fat content in the liver non-invasively [21, 33].

The diagnostic potential of SoS for quantifying hepatic steatosis was recently observed in a pilot study by Dioguardi Burgio et al. [21]. For study cohorts considered in our work, they obtained an AUC ranging from 0.91 to 1.0, slightly worse than in our case (0.93 - 1.0). Their method, however, only provides an average liver SoS estimate and requires a manual correction of the subcutaneous layer thickness with assumed SoS values to avoid biases [19, 22]. Furthermore, the US acquisition needs to carefully avoid the presence of large hepatic vessels and place the probe parallel to the liver capsule [21]. In comparison, CUTE is more efficient and provides a complete picture of the tissue composition through

spatially resolved SoS images. This information is crucial to extend the clinical use of CUTE beyond the assessment of hepatic steatosis and honor the versatility of US imaging modalities. For instance, in liver applications, CUTE-SoS images can help identify focal liver lesions such as liver adenomas and hepatocellular carcinoma. In principle, CUTE can image any organ accessible to pulse-echo US, and its clinical applications may also extend to breast cancer diagnosis [34, 35, 36] or the assessment of musculoskeletal disorders [37, 20], where SoS has already proven to be clinically relevant. Furthermore, CUTE-SoS images can also be used to correct aberrations in conventional B-mode images and improve their quality [38].

We provide preliminary evidence on the clinical value of CUTE in a single-center study with a relatively small and homogeneous study population. While being beyond the scope of this study, a larger and more diverse population would allow us to analyze the effects, if any, of confounding variables on CUTE-SoS estimates. Patients with significant steatosis were identified using indirect measurements to avoid unnecessary biopsies. Hence, uncertainties may exist in their diagnosis, although we expect them to be minimal given the expected good diagnostic performance of CAP in the studied cohort. Repeated CUTE-SoS measurements showed excellent correlation and agreement between them. However, careful repeatability and reproducibility analysis is still needed to understand measurement variability comprehensively.

In conclusion, CUTE offers a new quantitative imaging modality adapted to clinical US systems with high diagnostic value for screening for NAFLD cost-efficiently and non-invasively. It can be routinely performed together with the conventional US exploration with no additional cost for the practitioner, helping to tackle the high clinical burden that the increasing prevalence of NAFLD involves.

Methods

Study design and participants

This phase II, single-center, prospective, cross-sectional study was conducted at the Department for Visceral Surgery and Medicine at the University Hospital of Bern (Inselspital Bern, Switzerland) between August 2021 and November 2021. We recruited 22 patients that showed CAP values above 280 dB/m (significant or severe steatosis) during a regular screening visit at our center and 22 healthy individuals with no history of pre-existing liver conditions. All participants provided written informed consent in compliance with the principles of the Declaration of Helsinki and Good Clinical Practice. The study was approved by the Bern Cantonal Ethics Committee (ID 2020-03041). Study data were collected and managed using REDCap (Research Electronic Data Capture) hosted at the University of Bern [39, 40]. REDCap is a secure, web-based software platform designed to support data capture for research studies.

CAP measurements used in the study were acquired in a second visit and were supported with conventional US exploration to confirm the diagnosis. We collected US radio-frequency signals required for CUTE-SoS analysis immediately after the US exploration of each participant. A single physician experienced in US performed the data acquisition following a standardized acquisition protocol, with participants in the supine position, fasting state, and after at least five minutes of rest. Measurements corresponded to the right lobe liver parenchyma in the intercostal space. Although we integrated the CUTE-SoS imaging technology into the US system for clinical use, the physician was guided by conventional B-mode images and blinded to SoS images during the acquisition of US radio-frequency signals. These signals were stored in the US system and used for CUTE-SoS reconstructions by a researcher blinded to characteristics of participants and CAP values.

CAP measurements

We measured CAP values using the FibroScan 502 Touch (Echosens, Paris, France) transient elastography system with either the M or XL probe, which is automatically suggested by the device depending on the skin-to-capsule distance. The system provided the median (in dB/m) and inter-quantile range of a total of ten valid CAP measurements.

Ultrasound system

The conventional US exploration and the data acquisition for CUTE-SoS imaging were performed using the SuperSonic® MACH® 30 US system (Hologic® - Supersonic Imagine®, Aix en Provence, France) with the C6-1X convex probe. It has a center frequency of 3.46 MHz, a curvature radius of 60.34 mm, and 192 transducer elements with 0.336 mm pitch size. We used a Matlab-based framework (R2020b, MathWorks Inc., Natick, Massachusetts, USA) on a host computer to set up the parameters defining the scan sequence of ultrasound transmission and signal reception. Loading of these parameters to the US system, triggering execution of the scan sequence, and raw data transfer back to the host computer was done via Ethernet connection. A dedicated graphical user interface was created on the host computer to visualize simultaneously the echo-intensity B-mode and CUTE-SoS images reconstructed from the transferred data using a Matlab implementation of the CUTE software. This data transfer and image reconstruction took approximately 20 seconds per acquisition. Since the physician collecting US radio-frequency signals was guided by conventional B-mode images and blinded to SoS images, we stored the data on the computer for an off-line SoS reconstruction. Five acquisitions were taken per participant.

CUTE-SoS imaging

We transmitted sequentially 81 defocused wavefronts following a linear time delay law with steering angles relative to the aperture surface normal ranging from $-40°$ to $40°$ with $1°$ angle step. This linear delay law was equivalent to the one required for transmitting plane waves using linear probes [26] and generates therefore divergent waves in convex probes. We collected complex radio-frequency signals (analytic signals) at every transducer element for each transmit angle and reconstructed the corresponding complex radio-frequency images using delay-and-sum beamforming with assumed constant tissue SoS of 1555 m/s (Fig. 1a). The images were synthetically focused on transmission using coherent compounding to reduce clutter and to transform them to a set of images with transmit angles relative to the axial direction ranging from $-55°$ to $55°$ with $2.5°$ angle step. Each resulting image was again transformed into another set of synthetically steered images in reception using spatial frequency domain filtering [25] and the same sequence of angles as in transmission (Fig. 1c). In this way, we obtained an image per each angle pair in transmission and reception. We determined the spatial distribution of echo phase shifts using zero-lag complex cross-correlation between images of successive angle pairs with identical mid angle (Fig. 1d). Finally, we related the echo phase shift and tissue SoS at every spatial location assuming straight-ray propagation of US waves. The estimation of SoS from echo phase-shift measurements involves an ill-posed linear inverse problem; thus, we used zero- and first-order Tikhonov regularization to ensure meaningful solutions (Fig. 1e). The reader is referred to [26] for further details about the technical aspects and implementation of the method.

Statistical analysis

Statistical analysis and visualization were performed using Python (version 3.7.11) with the SciPy (1.6.2), Pandas (1.3.1), Seaborn (0.11.2), Pingouin (0.5.1), and Scikit-learn (1.0.1) libraries. Descriptive statistics including the mean, median, standard deviation, minimum and maximum values were used to summarize continuous variables, and frequencies and percentages were used for categorical variables. Here, we applied a two-tailed independent t-test to analyze the mean differences between two groups. The non-parametric two-sided Mann-Whitney U test was used to analyze the statistical significance of differences in distributions of CUTE-SoS and CAP in normal and steatotic livers. The correlation between CAP and CUTE-SoS measurements was calculated with the Pearson correlation coefficient. The degree of correlation and agreement between repeated CUTE-SoS measurements was assessed by the intraclass correlation coefficient using two-way random-effects model, average measure, and absolute agreement [41]. Results were considered significant for p-values lower than 0.05. The sensitivity and specificity of CUTE-SoS in predicting significant steatosis were analyzed using the area under the receiver operating characteristic (ROC) curve (AUC), with uncertainties computed by bootstrapping over 1000 realizations. The optimal SoS cut-off was determined by maximizing the geometric mean of the sensitivity and specificity.

Data availability

Data supporting the statistical analysis in this article is accessible within the manuscript and its Supplementary Information. Anonymized ultrasound raw datasets collected and analyzed during this study are available from the corresponding author upon request. However, data containing identifiable patient information is considered confidential, and disclosure to third parties is prohibited.

Acknowledgements

The authors would like to greatly thank all the subjects involved in this study for their valuable support. We also thank Hologic® - Supersonic Imagine®, Aix en Provence, France, for providing ultrasound imaging equipment, Thomas Frappart for technical assistance, and Prof. Jeffrey C. Bamber at the Institute of Cancer Research in London, UK, for inspiration and helpful discussions. This research has been funded by the Swiss National Science Foundation under project no. 205320_179038.

Author contributions

P.S. and M.J. adapted and integrated CUTE into the clinical US system and assisted with the study design. P.S. developed the graphical user interface for CUTE, performed CUTE-SoS reconstructions, and extracted liver SoS values. C.B. and A.B. assisted with the study design, recruited study participants, and performed CAP and US measurements. N.K.M. and P.S. analyzed the data, interpreted the results, wrote the manuscript, and made the figures. M.F. was the Principal Investigator for the study and is its guarantor. All authors provided critical comment, edited the manuscript, and approved its final version.

Competing interests

The authors declare no competing interests.

References

[1] S. Bellentani, "The epidemiology of non-alcoholic fatty liver disease," *Liver international*, vol. 37, pp. 81–84, 2017.

[2] G. Bedogni, L. Miglioli, F. Masutti, A. Castiglione, L. S. Croce, C. Tiribelli, and S. Bellentani, "Incidence and natural course of fatty liver in the general population: the Dionysos study," *Hepatology*, vol. 46, no. 5, pp. 1387–1391, 2007.

[3] A. Wieckowska and A. E. Feldstein, "Diagnosis of nonalcoholic fatty liver disease: invasive versus noninvasive," in *Seminars in liver disease*, vol. 28, pp. 386–395, © Thieme Medical Publishers, 2008.

[4] G. Targher, C. P. Day, and E. Bonora, "Risk of cardiovascular disease in patients with nonalcoholic fatty liver disease," *New England Journal of Medicine*, vol. 363, no. 14, pp. 1341–1350, 2010.

[5] A. Berzigotti, E. Tsochatzis, J. Boursier, L. Castera, N. Cazzagon, M. Friedrich-Rust, S. Petta, and M. Thiele, "EASL Clinical Practice Guidelines on non-invasive tests for evaluation of liver disease severity and prognosis – 2021 update," *Journal of Hepatology*, vol. 75, no. 3, pp. 659–689, 2021.

[6] G. Ferraioli and L. B. Soares Monteiro, "Ultrasound-based techniques for the diagnosis of liver steatosis," *World journal of gastroenterology*, vol. 25, no. 40, pp. 6053–6062, 2019.

[7] G. Ferraioli, A. Berzigotti, R. G. Barr, B. I. Choi, X. W. Cui, Y. Dong, O. H. Gilja, J. Y. Lee, D. H. Lee, F. Moriyasu, F. Piscaglia, K. Sugimoto, G. L.-H. Wong, V. W.-S. Wong, and C. F. Dietrich, "Quantification of Liver Fat Content with Ultrasound: A WFUMB Position Paper," *Ultrasound in Medicine & Biology*, vol. 47, no. 10, pp. 2803–2820, 2021.

[8] W. J. Zwiebel, "Sonographic diagnosis of diffuse liver disease," in *Seminars in Ultrasound, CT and MRI*, vol. 16, pp. 8–15, Elsevier, 1995.

[9] S. Dasarathy, J. Dasarathy, A. Khiyami, R. Joseph, R. Lopez, and A. J. McCullough, "Validity of real time ultrasound in the diagnosis of hepatic steatosis: a prospective study," *Journal of hepatology*, vol. 51, no. 6, pp. 1061–1067, 2009.

[10] J. R. van Werven, H. A. Marsman, A. J. Nederveen, N. J. Smits, F. J. ten Kate, T. M. van Gulik, and J. Stoker, "Assessment of Hepatic Steatosis in Patients Undergoing Liver Resection: Comparison of US, CT, T1-weighted Dual-Echo MR Imaging, and Point-resolved 1H MR Spectroscopy," *Radiology*, vol. 256, no. 1, pp. 159–168, 2010. PMID: 20574093.

[11] K. Suzuki, N. Hayashi, Y. Sasaki, M. Kono, A. Kasahara, H. Fusamoto, Y. Imai, and T. Kamada, "Dependence of ultrasonic attenuation of liver on pathologic fat and fibrosis: Examination with experimental fatty liver and liver fibrosis models," *Ultrasound in Medicine & Biology*, vol. 18, no. 8, pp. 657–666, 1992.

[12] M. Sasso, M. Beaugrand, V. de Ledinghen, C. Douvin, P. Marcellin, R. Poupon, L. Sandrin, and V. Miette, "Controlled Attenuation Parameter (CAP): A Novel VCTE™ Guided Ultrasonic Attenuation Measurement for the Evaluation of Hepatic Steatosis: Preliminary Study and Validation in a Cohort of Patients with Chronic Liver Disease from Various Causes," *Ultrasound in Medicine & Biology*, vol. 36, no. 11, pp. 1825–1835, 2010.

[13] M. Sasso, S. Audière, A. Kemgang, F. Gaouar, C. Corpechot, O. Chazouillères, C. Fournier, O. Golsztejn, S. Prince, Y. Menu, L. Sandrin, and V. Miette, "Liver Steatosis Assessed by Controlled Attenuation Parameter (CAP) Measured with the XL Probe of the FibroScan: A Pilot Study Assessing Diagnostic Accuracy," *Ultrasound in Medicine & Biology*, vol. 42, no. 1, pp. 92–103, 2016.

[14] S. Baumeler, W. Jochum, J. Neuweiler, I. Bergamin, and D. Semela, "Controlled attenuation parameter for the assessment of liver steatosis in comparison with liver histology: a single-centre real life experience," *Swiss medical weekly*, vol. 149, no. 1718, 2019.

[15] P. J. Eddowes, M. Sasso, M. Allison, E. Tsochatzis, Q. M. Anstee, D. Sheridan, I. N. Guha, J. F. Cobbold, J. J. Deeks, V. Paradis, *et al.*, "Accuracy of FibroScan controlled attenuation parameter and liver stiffness measurement in assessing steatosis and fibrosis in patients with nonalcoholic fatty liver disease," *Gastroenterology*, vol. 156, no. 6, pp. 1717–1730, 2019.

[16] D. Petroff, V. Blank, P. N. Newsome, Shalimar, C. S. Voican, M. Thiele, V. de Lédinghen, S. Baumeler, W. K. Chan, G. Perlemuter, A.-C. Cardoso, S. Aggarwal, M. Sasso, P. J. Eddowes, M. Allison, E. Tsochatzis, Q. M. Anstee, D. Sheridan, J. F. Cobbold, S. Naveau, M. Lupsor-Platon, S. Mueller, A. Krag, M. Irles-Depe, D. Semela, G. L.-H. Wong, V. W.-S. Wong, C. A. Villela-Nogueira, H. Garg, O. Chazouillères, J. Wiegand, and T. Karlas, "Assessment of hepatic steatosis by controlled attenuation parameter using the M and XL probes: an individual patient data meta-analysis," *The Lancet Gastroenterology & Hepatology*, vol. 6, no. 3, pp. 185–198, 2021.

[17] T. Karlas, D. Petroff, M. Sasso, J.-G. Fan, Y.-Q. Mi, V. de Lédinghen, M. Kumar, M. Lupsor-Platon, K.-H. Han, A. C. Cardoso, G. Ferraioli, W.-K. Chan, V. W.-S. Wong, R. P. Myers, K. Chayama, M. Friedrich-Rust, M. Beaugrand, F. Shen, J.-B. Hiriart, S. K. Sarin, R. Badea, K. S. Jung, P. Marcellin, C. Filice, S. Mahadeva, G. L.-H. Wong, P. Crotty, K. Masaki, J. Bojunga, P. Bedossa, V. Keim, and J. Wiegand, "Individual patient data meta-analysis of controlled attenuation parameter (CAP) technology for assessing steatosis," *Journal of Hepatology*, vol. 66, no. 5, pp. 1022–1030, 2017.

[18] F. A. Duck, "Chapter 4 - Acoustic Properties of Tissue at Ultrasonic Frequencies," in *Physical Properties of Tissues* (F. A. Duck, ed.), pp. 73–135, London: Academic Press, 1990.

[19] M. Imbault, A. Faccinetto, B.-F. Osmanski, A. Tissier, T. Deffieux, J.-L. Gennisson, V. Vilgrain, and M. Tanter, "Robust sound speed estimation for ultrasound-based hepatic steatosis assessment," *Physics in Medicine and Biology*, vol. 62, no. 9, p. 3582, 2017.

[20] L. Ruby, A. Kunut, D. N. Nakhostin, F. A. Huber, T. Finkenstaedt, T. Frauenfelder, S. J. Sanabria, and M. B. Rominger, "Speed of sound ultrasound: comparison with proton density fat fraction assessed with Dixon MRI for fat content quantification of the lower extremity," *European Radiology*, vol. 30, no. 10, p. 5272, 2020.

[21] M. D. Burgio, M. Imbault, M. Ronot, A. Faccinetto, B. E. Van Beers, P.-E. Rautou, L. Castera, J.-L. Gennisson, M. Tanter, and V. Vilgrain, "Ultrasonic adaptive sound speed estimation for the diagnosis and quantification of hepatic steatosis: a pilot study," *Ultraschall in der Medizin-European Journal of Ultrasound*, vol. 40, no. 06, pp. 722–733, 2019.

[22] M. Imbault, M. D. Burgio, A. Faccinetto, M. Ronot, H. Bendjador, T. Deffieux, E. O. Triquet, P.-E. Rautou, L. Castera, J.-L. Gennisson, *et al.*, "Ultrasonic fat fraction quantification using in vivo adaptive sound speed estimation," *Physics in Medicine & Biology*, vol. 63, no. 21, p. 215013, 2018.

[23] M. Jaeger, G. Held, S. Peeters, S. Preisser, M. Grünig, and M. Frenz, "Computed ultrasound tomography in echo mode for imaging speed of sound using pulse-echo sonography: proof of principle," *Ultrasound in medicine and biology*, vol. 41, no. 1, pp. 235–250, 2015.

[24] M. Jaeger and M. Frenz, "Towards clinical computed ultrasound tomography in echo-mode: Dynamic range artefact reduction," *Ultrasonics*, vol. 62, pp. 299–304, 2015.

[25] P. Stähli, M. Kuriakose, M. Frenz, and M. Jaeger, "Improved forward model for quantitative pulse-echo speed-of-sound imaging," *Ultrasonics*, p. 106168, 2020.

[26] M. Jaeger, P. Stähli, N. Korta Martiartu, P. Salemi Yolgunlu, T. Frappart, C. Fraschini, and M. Frenz, "Pulse-echo speed-of-sound imaging using convex probes," 2022.

[27] P. Stähli, M. Frenz, and M. Jaeger, "Bayesian Approach for a Robust Speed-of-Sound Reconstruction Using Pulse-Echo Ultrasound," *IEEE transactions on medical imaging*, vol. 40, no. 2, pp. 457–467, 2020.

[28] G. Ferraioli, C. Filice, L. Castera, B. I. Choi, I. Sporea, S. R. Wilson, D. Cosgrove, C. F. Dietrich, D. Amy, J. C. Bamber, R. Barr, Y.-H. Chou, H. Ding, A. Farrokh, M. Friedrich-Rust, T. J. Hall, K. Nakashima, K. R. Nightingale, M. L. Palmeri, F. Schafer, T. Shiina, S. Suzuki, and M. Kudo, "WFUMB Guidelines and Recommendations for Clinical Use of Ultrasound Elastography: Part 3: Liver," *Ultrasound in Medicine & Biology*, vol. 41, no. 5, pp. 1161–1179, 2015.

[29] M. Kuriakose, J.-W. Muller, P. Stähli, M. Frenz, and M. Jaeger, "Receive Beam-Steering and Clutter Reduction for Imaging the Speed-of-Sound Inside the Carotid Artery," *Journal of Imaging*, vol. 4, no. 12, p. 145, 2018.

[30] C. Sehgal, G. Brown, R. Bahn, and J. Greenleaf, "Measurement and use of acoustic nonlinearity and sound speed to estimate composition of excised livers," *Ultrasound in Medicine & Biology*, vol. 12, no. 11, pp. 865–874, 1986.

[31] J. C. Bamber and C. Hill, "Ultrasonic attenuation and propagation speed in mammalian tissues as a function of temperature," *Ultrasound in Medicine and Biology*, vol. 5, no. 2, pp. 149–157, 1979.

[32] T. Lin, J. Ophir, and G. Potter, "Correlations of Sound Speed with Tissue Constituents in Normal and Diffuse Liver Disease," *Ultrasonic Imaging*, vol. 9, no. 1, pp. 29–40, 1987. PMID: 3299967.

[33] A. V. Telichko, R. Ali, T. Brevett, H. Wang, J. G. Vilches-Moure, S. U. Kumar, R. Paulmurugan, and J. J. Dahl, "Noninvasive estimation of local speed of sound by pulse-echo ultrasound in a rat model of nonalcoholic fatty liver," *Physics in Medicine & Biology*, vol. 67, p. 015007, jan 2022.

[34] L. Ruby, S. J. Sanabria, K. Martini, K. J. Dedes, D. Vorburger, E. Oezkan, T. Frauenfelder, O. Goksel, and M. B. Rominger, "Breast Cancer Assessment With Pulse-Echo Speed of Sound Ultrasound From Intrinsic Tissue Reflections: Proof-of-Concept," *Investigative radiology*, vol. 54, no. 7, pp. 419–427, 2019.

[35] R. Natesan, J. Wiskin, S. Lee, and B. H. Malik, "Quantitative assessment of breast density: transmission ultrasound is comparable to mammography with tomosynthesis," *Cancer Prevention Research*, vol. 12, no. 12, pp. 871–876, 2019.

[36] N. Duric, M. Sak, S. Fan, R. M. Pfeiffer, P. J. Littrup, M. S. Simon, D. H. Gorski, H. Ali, K. S. Purrington, R. F. Brem, M. E. Sherman, and G. L. Gierach, "Using Whole Breast Ultrasound Tomography to Improve Breast Cancer Risk Assessment: A Novel Risk Factor Based on the Quantitative Tissue Property of Sound Speed," *Journal of Clinical Medicine*, vol. 9, no. 2, 2020.

[37] S. J. Sanabria, K. Martini, G. Freystätter, L. Ruby, O. Goksel, T. Frauenfelder, and M. B. Rominger, "Speed of sound ultrasound: a pilot study on a novel technique to identify sarcopenia in seniors," *European Radiology*, vol. 29, no. 1, pp. 3–12, 2019.

[38] M. Jaeger, E. Robinson, H. G. Akarçay, and M. Frenz, "Full correction for spatially distributed speed-of-sound in echo ultrasound based on measuring aberration delays via transmit beam steering," *Physics in medicine & biology*, vol. 60, no. 11, p. 4497, 2015.

[39] P. A. Harris, R. Taylor, R. Thielke, J. Payne, N. Gonzalez, and J. G. Conde, "Research electronic data capture (REDCap)—A metadata-driven methodology and workflow process for providing translational research informatics support," *Journal of Biomedical Informatics*, vol. 42, no. 2, pp. 377–381, 2009.

[40] P. A. Harris, R. Taylor, B. L. Minor, V. Elliott, M. Fernandez, L. O'Neal, L. McLeod, G. Delacqua, F. Delacqua, J. Kirby, and S. N. Duda, "The REDCap consortium: Building an international community of software platform partners," *Journal of Biomedical Informatics*, vol. 95, p. 103208, 2019.

[41] T. K. Koo and M. Y. Li, "A Guideline of Selecting and Reporting Intraclass Correlation Coefficients for Reliability Research," *Journal of Chiropractic Medicine*, vol. 15, no. 2, pp. 155–163, 2016.

Supplementary Files

This is a list of supplementary files associated with this preprint. Click to download.

- SupplementaryInformation.pdf